Journal of Plankton Research, 2025, **47**, fbae066
https://doi.org/10.1093/plankt/fbae066
Advance access publication date 23 December 2024
Original Article

Mixotrophs and Mixoplankton: Conceptual Integration into Aquatic Research

Predictable shifts from nutrient to energy limitation determine the responses of planktonic autotrophs, bacteria and mixoplankton to browning

Sierra Cagle[1] and Sebastian Diehl[2]

[1]Department of Marine Biology, Texas A&M University, 200 Seawolf Pkwy, Galveston, TX 77554, USA
[2]Integrated Science Lab, Department of Ecology and Environmental Science, Umeå University, SE-90187 Umeå, Sweden

*Corresponding author: SEC1414@tamu.edu

Corresponding editor: Beatrix E. Beisner

ABSTRACT

Within aquatic ecosystems, heterotrophic, mixotrophic and autotrophic plankton are entangled in a complex network of competitive, predatory and mutualistic interactions. "Browning," the increase of colored dissolved organic matter (CDOM) from terrestrial catchments, can affect this network of interactions by simultaneously decreasing light availability and increasing organic carbon and nutrients supplies. Here, we introduce a conceptual, process-based numerical model to investigate the effects of browning on a microbial food web consisting of heterotrophic bacterioplankton, bacterivorous phago-mixoplankton, autotrophic phytoplankton and the resources light, inorganic phosphorus and DOM. Additionally, we explore how the investment in autotrophic vs. phagotrophic resource acquisition influences mixoplankton performance. Several model predictions are in broad agreement with empirical observations under increasing CDOM supply, including increased bacterial biomass and inorganic phosphorous, decreased light penetration, the potential for a unimodal phytoplankton biomass response and a local minimum in mixoplankton biomass. Our results also suggest that mixoplankton with a high investment in phototrophy perform best in many conditions but that phosphorous acquisition via prey is crucial under high light-low nutrient conditions. Overall, our model analyses suggest that responses to altered CDOM supply are largely determined by systematic changes in the relative importance of nutrient vs. energy limitation of each plankton group.

KEYWORDS: plankton network; mixoplankton; primary production; browning; CDOM; terrestrial carbon; dissolved organic carbon

INTRODUCTION

In many areas, fluxes of "colored" dissolved organic material (CDOM) to aquatic ecosystems from the surrounding watershed have been impacted by climate change and anthropogenic activities altering land cover (Kritzberg *et al.*, 2020; Blanchet *et al.*, 2022; Räike *et al.*, 2024). Importantly, elevated CDOM levels increase attenuation of photosynthetically active radiation (PAR, 400–700 nm) within the water column, altering the light regime, a phenomenon termed "coastal darkening" or "brownification." The influx of organic material can also act as a carbon or nutrient subsidy depending on the source and molecular structure of the material, which determines how bioavailable it is to microbial populations (Klug, 2005; Kritzberg *et al.*, 2006). Importantly, altered resource regimes from increased CDOM loading can impact planktonic bacteria and primary producers with the potential to shift community structure and ecosystem functioning (Jones, 1998; Jansson *et al.*, 2000; Williamson *et al.*, 2015; Mustaffa *et al.*, 2020; Senar *et al.*, 2021). Further, reductions in biomass of higher trophic levels have been reported to occur in systems where increased CDOM levels were correlated with reduced biomass of primary producers (Karlsson *et al.*, 2015).

Previous research has suggested a unimodal relationship between primary production and dissolved organic carbon (DOC), the primary component of CDOM (Seekell *et al.*, 2015a). This pattern is driven by the positive effect of low DOC concentrations through nutrient subsidy up to the point where the negative effect of light limitation prevails (Seekell *et al.*, 2015b). CDOM-associated nutrients are made available to primary producers through photochemical and microbial processes. Bacterioplankton are important degraders of CDOM, with the ability to indirectly stimulate primary productivity by acting as net nutrient mineralizers; however, they can also suppress primary productivity under resource conditions that shift their role to net nutrient competitors (Joint *et al.*, 2002; Klug, 2005). This relationship is mediated by bacterioplankton resource preferences. In general, labile sources of carbon and phosphorous are more readily taken up than recalcitrant CDOM-associated resources. Further intertwining associations between these planktonic groups, primary producers generate a pool of highly bioavailable carbon that can serve as an important energy source for bacterioplankton (Baines and Pace, 1991). CDOM-related shifts in these processes and relationships have important implications for energy and nutrient fluxes within

Received: June 4, 2024. **Editorial decision:** October 21, 2024. **Accepted:** October 23, 2024

aquatic ecosystems (Cotner and Biddanda, 2002; Karlsson *et al.*, 2015).

The group of organisms considered planktonic primary producers are characterized by a range of trophic strategies, from pure autotrophic resource acquisition (autotrophic phytoplankton) to a mix of autotrophic and phago-heterotrophic resource acquisition (bacterivorous phago-mixoplankton). Historically underrepresented in ecological studies, mixoplankton are of considerable interest when attempting to elucidate the effects of CDOM on aquatic ecosystems, as their trophic strategy generates linkages between bacterial production and potential primary productivity. In many aquatic systems, both clear water and highly CDOM impacted, the common occurrence and importance of mixotrophic flagellates are well established (Flynn *et al.*, 2013; Mitra *et al.*, 2014; Selosse *et al.*, 2017; Stoecker *et al.*, 2017; Le Noac'h *et al.*, 2024), along with their potential to exert a strong top-down control on bacterioplankton (Šimek *et al.*, 2001; Schmidtke *et al.*, 2006; Unrein *et al.*, 2007). Further, DOC has been shown to indirectly stimulate mixotroph populations through increased bacterial prey production (Wilken *et al.*, 2018). The ability of mixoplankton to obtain nutrients through multiple pathways (uptake of dissolved inorganics and phagotrophy of bacterial prey) may allow them to better withstand the reduced light conditions associated with browning and to some extent, compensate for reductions in primary productivity by more heavily light dependent autotrophs. However, studies have suggested the importance of light as a mediator of bacterivory in mixoplankton (Ptacnik *et al.*, 2016; Fischer *et al.*, 2017) and the significance of synergisms between photosynthetic carbon fixation and inorganic phosphorous acquired via predation (Mitra and Flynn, 2023). Therefore, it is still unclear how these highly connected networks of microbes may be impacted by browning.

In work presented here, we use a conceptual, process-based model to investigate how a network of autotrophic phytoplankton, mixoplankton and bacterioplankton responds to a gradient of CDOM and phosphorous loading and how these responses are mediated by resource dynamics. Additionally, we consider how the mixoplankton's relative investment in autotrophic vs. phagotrophic resource acquisition influences model dynamics. As alterations in CDOM and nutrient supply to aquatic ecosystems are ongoing in many regions, understanding how these processes influence plankton networks is critical for evaluation of potential climate change impacts and development of resource management strategies for environments in flux.

METHODS

Model description

To address our study questions related to the influence of resource supply on plankton network interactions, we extend and analyze a conceptual, process-based model describing the dynamics of autotrophic phytoplankton, phago-mixotrophic phytoplankton (hereafter called mixoplankton) and heterotrophic bacterioplankton Le Noac'h *et al.*, 2025). The model is process-based in that it explicitly describes the consumption and regeneration of four energy and nutrient sources that are potentially growth-limiting to one or more plankton populations, i.e. solar irradiance, labile organic carbon, CDOM and mineral phosphorus (Fig. 1). The model is conceptual in that it makes a number of simplifying assumptions about resource acquisition, transformation and regeneration, such as fixed phosphorus:carbon ratios of organismal biomass, discrete switches between energy and nutrient limitation of growth along resource gradients and instant mineralization of dead biomass and excreted organic nutrients. The model thus sacrifices physiological detail for analytical tractability and the possibility to gain general, conceptual understanding of the mechanisms that drive system responses to the investigated environmental drivers, i.e. external input of CDOM and mineral nutrients.

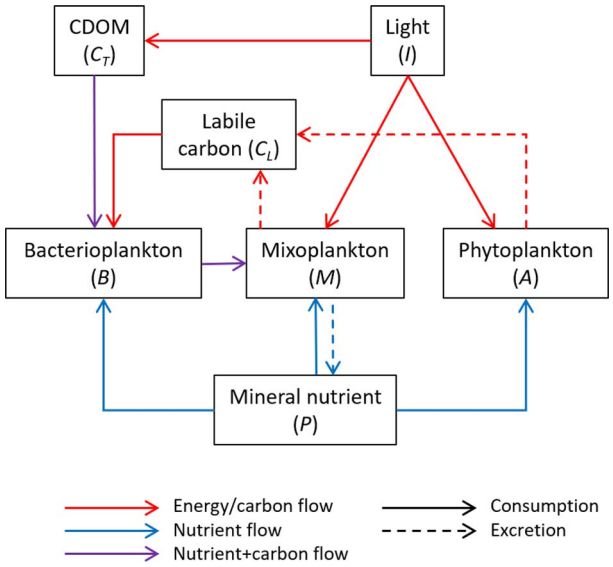

Fig. 1. Model structure where processes include: (i) attenuation of light (I) by terrestrial CDOM (C_T); (ii) attenuation and consumption of light energy for carbon fixation by autotrophic phytoplankton (A) and mixoplankton (M); (iii) excretion of labile carbon (C_L) by autotrophic phytoplankton and mixoplankton due to excess photosynthetic product under nutrient limitation; (iv) consumption of mineral nutrient (P) by heterotrophic bacterioplankton (B), mixoplankton and autotrophic phytoplankton; (v) excretion of excess mineral nutrient by mixoplankton under energy limitation; (vi) consumption of bacteria by mixoplankton; (vii) consumption of labile carbon by bacteria; and (viii) consumption of terrestrial CDOM by bacteria.

The model

The model describes the rates of change of the following state variables in a well-mixed water column with uniform depth (z_{max}): irradiance (I), the carbon biomasses of autotrophic phytoplankton (A), mixoplankton (M) and heterotrophic bacterioplankton (B), the concentrations of labile (C_L) and CDOM carbon (C_T) and the concentration of dissolved inorganic phosphorous (P). The dynamics of these state variables are described with differential equations and solved using MATLAB's function for stiff ordinary differential equations (version 2021b, ode15, error tolerance 1e-9). Model equations are listed in Table I and a list of symbols, definitions, values and units of the state variables and parameters is provided in Table II.

The processes incorporated into these equations are described below and summarized in Fig. 1.

Four of the state variables experience influxes from outside. Irradiance enters the water surface with incoming intensity I_0, while inorganic phosphorus, CDOM and bacteria enter the water column proportional to the water exchange rate D/z_{max} and the incoming concentrations P_{in}, $C_{T_{in}}$ and B_{in}, respectively. Irradiance (Table I, equation (1)) is attenuated vertically by phytoplankton, mixoplankton, CDOM and water with attenuation coefficients k_A, k_M, k_T and k_W, respectively, where attenuation by mixoplankton is proportional to the autotrophic investment, α, described below. All other state variables (A, M, B, C_T, C_L and P) are lost from the system at the water exchange rate D/z_{max}. The plankton populations experience additional losses proportional to their combined metabolic and mortality loss rates (l_A, l_M or l_B).

The growth of all three populations can be either energy or nutrient-limited, as described by minimum functions of their specific growth rates. Note that in cases where bacterial and mixoplankton growth is nutrient-limited, we assume that heterotrophically acquired organic nutrients are converted into growth without losses, whereas only a fraction of ingested carbon is converted into energy limited growth to account for the energetic costs of growth.

The specific growth rate of autotrophs is defined as the minimum of either the light or mineral phosphorus-dependent growth rate integrated over the depth of the water column (Table I , equation (2)). Both growth rates are described by Monod terms (Monod, 1949) with maximum growth rate (p_A), resource concentration (I or P) and a half saturation constant (H_A *or* S_{PA}, respectively), where the integral over the vertical light gradient is solved explicitly (Table I, equation (2)).

Similarly, the specific growth rate of mixoplankton is defined as the minimum of either the energy or phosphorus-dependent growth rate, where (photosynthetic) energy and mineral nutrients are acquired in the same way as by autotrophs, but also through ingestion of bacteria (Table I, equation (3)). The energy-dependent growth rate is thus the combination of growth from photosynthesis and ingestion of bacterial carbon, while the phosphorus dependent growth rate is the combination of growth from mineral phosphorus uptake and ingestion of bacterial phosphorus. The relative importance of these pathways depends on the mixoplankton's fractional investment α into phototrophy and mineral nutrient uptake, and the reverse fractional investment $(1–\alpha)$ into phago-heterotrophy, as well as on the conversion efficiencies of ingested bacterial carbon c_{BM} and phosphorus q_B/q_M into mixoplankton growth (where q_B and q_M are the phosphorus:carbon ratios of bacteria and mixoplankton). The ingestion of bacteria itself is described by a type 3 functional response (Wilken *et al.*, 2010; Principiotta *et al.*, 2016; Ghyoot *et al.*, 2017) with maximum ingestion rate J_{BM} and half saturation constant S_{BM}.

Finally, bacterial growth is also defined as the minimum of energy or phosphorus-dependent growth. Bacteria obtain energy from labile carbon and CDOM, while phosphorous substrates include mineral phosphorus and organic phosphorous associated with CDOM (Table I, See equation (4)). Carbon substrates are ingested with maximum rates J_{LB} for labile carbon and $f_T J_{LB}$ for CDOM, half saturation constant S_{CB} and converted into bacterial growth with efficiencies c_{LB} and c_{TB}, respectively. We assume $f_T < 1$ and $c_{TB} < c_{LB}$ to account for the recalcitrant nature of CDOM making it more difficult to take up and metabolize. Phosphorus is ingested in mineral form with maximum rate J_{PB} and half saturation constant S_{PB} and in organic form as a fraction q_T of the ingested CDOM, both of which are converted into the phosphorus dependent bacterial growth rate proportionally to the bacterial carbon:phosphorus ratio $1/q_B$. In addition to losses from dilution, metabolism and background mortality, bacteria experience losses from predation by mixoplankton, as described in the previous paragraph.

The rate of change of the mineral phosphorus concentration is the balance of external inputs minus losses from dilution at rate D/z_{max}, instant recycling from organismal background mortality and metabolism, as well as uptake and/or excretion by plankton organisms (Table I, equation (5)). While the minimum functions in equation (5) look complex, they represent the net effects on mineral nutrient uptake or excretion of the above-described growth processes and therefore contain only familiar functions and parameters. Thus, while autotrophs always take up mineral phosphorus in proportion to their (energy or nutrient-limited) growth rate, bacteria and mixoplankton do so only when their growth is phosphorus-limited. When growth is energy limited, bacteria and mixoplankton take up more organic phosphorus from assimilated CDOM and ingested bacteria, respectively, than needed to complement their potential mineral nutrient uptake. This results in reduced mineral phosphorus uptake by bacteria and mixoplankton and sometimes even in a net excretion of re-mineralized surplus organic phosphorus.

The rate of change of the concentration of CDOM carbon is the balance of external inputs minus losses from dilution at rate D/z_{max}, as well as uptake by bacteria as described above (Table I, equation (6)). Because bacteria use CDOM both as a carbon and a nutrient source, this rate is the same whether bacteria are energy or phosphorus limited. In the former case, all CDOM carbon is used for growth, whereas in the latter case, any surplus carbon not needed for growth is respired.

The rate of change of the labile carbon concentration is the balance of excretion by autotrophs and mixoplankton, uptake by bacteria and dilution at rate D/z_{max} (Table I, equation (7)). We assume that autotrophs and mixotrophs excrete labile carbon only when their growth rates are nutrient-limited, in which case they excrete a fraction e_{AL} or e_{ML}, respectively, of their potential surplus carbon assimilation, in excess of their carbon needs for phosphorus limited growth. The remaining fraction ($1–e_{AL}$, $1–e_{ML}$) of this potential surplus assimilation is not accounted for, assuming that it is respired or not realized (through partial decoupling of photochemical reactions from carbon fixation). Finally, we assume that bacteria take up and assimilate labile carbon more easily than CDOM carbon. Thus, under nutrient-limited growth, when bacteria ingest CDOM to maximize their phosphorus uptake, they do not assimilate all of the accompanying carbon. Rather, they cover their carbon needs partly or entirely from uptake of labile carbon. In contrast, when bacterial growth is energy-limited, bacteria take up labile carbon at a rate $J_{LH}C_L/\left(C_L + f_T C_T + S_{CH}\right)$, as explained in the paragraph on bacterial growth.

Table I: *Differential and algebraic equations describing the dynamical system*

Light intensity at depth z_{max} (μmol photons m^{-2} s^{-1})	$I_{z_{max}} = I_0 e^{-(k_A A+\alpha k_M M+k_T C_T+K_W) z_{max}}$	1
Biomass of autotrophic phytoplankton ($g\,C/m^3$)	$\frac{dA}{dt} = \min\left[\frac{p_A}{z_{max}(k_A A+\alpha k_M M+k_T C_T+k_W)}\ln\left(\frac{I_0+H_A}{I_{z_{max}}+H_A}\right); p_A\frac{P}{P+S_{RA}}\right]A - l_A A - \frac{D}{z_{max}}A$	2
Biomass of mixoplankton ($g\,C/m^3$)	$\frac{dM}{dt} =$ $\min\left[\alpha\frac{p_M}{z_{max}(k_A A+\alpha k_M M+k_T C_T+k_W)}\ln\left(\frac{I_0+H_M}{I_{z_{max}}+H_M}\right) + c_{BM}(1-\alpha)J_{BM}\frac{B^2}{B^2+S_{BM}^2}; \alpha p_M\frac{P}{P+S_{PM}} + \frac{q_B}{q_M}(1-\alpha)J_{BM}\frac{B^2}{B^2+S_{BM}^2}\right]M -$ $l_M M - \frac{D}{z_{max}}M$	3
Biomass of heterotrophic bacterioplankton ($g\,C/m^3$)	$\frac{dB}{dt} = \min\left[J_{LB}\frac{c_{LB}C_L+c_{TB}f_T C_T}{C_L+f_T C_T+S_{CB}}; \frac{1}{q_B}\left(q_T J_{LB}\frac{f_T C_T}{C_L+f_T C_T+S_{CB}} + J_{PB}\frac{P}{P+S_{PB}}\right)\right]B - (1-\alpha)J_{BM}\frac{B^2}{B^2+S_{BM}^2}M - l_B B + \frac{D}{z_{max}}(B_{in}-B)$	4
Inorganic phosphorous concentration ($g\,P/m^3$)	$\frac{dP}{dt} = \frac{D}{z_{max}}(P_{in}-P) + q_A l_A A + q_M l_M M + q_B l_B B - \min\left[\frac{p_A}{z_{max}(k_A A+\alpha k_M M+k_T C_T+k_W)}\ln\left(\frac{I_0+B_A}{I_{z_{max}}+B_A}\right); p_A\frac{P}{P+S_{PA}}\right]q_A A -$ $\min\left[q_B J_{LB}\frac{c_{LB}C_L+c_{TB}f_T C_T}{C_L+f_T C_T+S_{CB}} - q_T J_{LB}\frac{f_T C_T}{C_L+f_T C_T+S_{CB}}; J_{PB}\frac{P}{P+S_{PB}}\right]B -$ $\min\left[\frac{q_M\alpha p_M}{z_{max}(k_A A+\alpha k_M M+k_T C_T+k_W)}\ln\left(\frac{I_0+B_M}{I_{z_{max}}+B_M}\right) + (q_M c_{BM} - q_B)(1-\alpha)J_{BM}\frac{B^2}{B^2+S_{BM}^2}; q_M\alpha p_M\frac{P}{P+S_{PM}}\right]M$	5
Terrestrial CDOM concentration ($g\,C/m^3$)	$\frac{dC_T}{dt} = \frac{C_T}{z_{max}}(C_{T\,in}-C_T) - J_{LB}\frac{f_T C_T}{C_L+f_T C_T+S_{CB}}B$	6
Labile carbon concentration ($g\,C/m^3$)	$\frac{dC_L}{dt} = e_{AL}\max\left[0; \frac{p_A}{z_{max}(k_A A+\alpha k_M M+k_T C_T+k_W)}\ln\left(\frac{I_0+B_A}{I_{z_{max}}+B_A}\right) - p_A\frac{R}{R+S_{RA}}\right]A +$ $e_{ML}\max\left[0; \alpha\frac{p_M}{z_{max}(k_A A+\alpha k_M M+k_T C_T+k_W)}\ln\left(\frac{I_0+B_M}{I_{z_{max}}+B_M}\right) + \left(c_{BM} - \frac{q_B}{q_M}\right)(1-\alpha)J_{BM}\frac{B^2}{B^2+S_{BM}^2} - \alpha p_M\frac{P}{P+S_{PM}}\right]M -$ $\min\left[J_{LB}\frac{C_L}{C_L+f_T C_T+S_{CB}}; \frac{1}{c_{LB}q_B}\left(q_T J_{LB}\frac{f_T C_T}{C_L+f_T C_T+S_{CB}} + J_{PB}\frac{P}{P+S_{PB}}\right)\right]B - \frac{D}{z_{max}}C_L$	7

State variables are defined (with units) in the left column and numbered as shown in the right column. Parameters are defined in Table II.

Table II: *Symbols, definitions, values and units of the state variables and parameters*

Variables/ parameters	Definition	Value	Units	Source or justification
A	Biomass of autotrophic phytoplankton		g C m^{-3}	
M	Biomass of phago-mixoplankton		g C m^{-3}	
B	Biomass of heterotrophic bacteria		g C m^{-3}	
$I(z)$	PAR at depth z		μmol photons m^{-2} s^{-1}	
P	Inorganic phosphorous concentration		g P m^{-3}	
C_L	Labile C concentration		g C m^{-3}	
C_T	Terrestrial CDOM concentration		g C m^{-3}	
α	Effort spent by mixotroph on photosynthesis and mineral nutrient uptake	$0 \leq \alpha \leq 1$	dimensionless	Fixed strategy (i.e. does not vary over time)
B_{in}	Concentration of bacteria in influx	0.001	g C m^{-3}	Set to a low value that stabilizes dynamics
c_{BM}	C conversion efficiency of mixotroph (feeding on bacteria)	0.5	Dimensionless	Personal communication
c_{LB}	Conversion efficiency of labile C by bacteria	0.5	Dimensionless	$c_{TB} < c_{LB}$ (CDOM is of lower quality than labile C)
c_{TB}	Conversion efficiency of CDOM-carbon by bacteria	0.3	Dimensionless	
C_{Tin}	Concentration of terrestrial CDOM in influx	0–120	g C m^{-3}	Possible range in nature
D	Water exchange rate coefficient	0.035	m d^{-1}	Yields a water residence time of ~30 days
e_{AL}	Fraction of potential surplus C production excreted as labile C by autotrophs	0.1	Dimensionless	Assumes that the realized surplus C production is 10%
e_{ML}	Fraction of potential surplus C production excreted as labile C by mixoplankton	0.1	Dimensionless	Potential surplus C production (when growth is nutrient-limited)
f_T	Uptake efficiency of CDOM by bacteria as a fraction of uptake efficiency of labile C	0.2	Dimensionless	Assumes that the uptake rate of large CDOM molecules is lower than the uptake rate of small labile carbon molecules
H_A	Half-saturation constant of light-dependent growth of autotrophs	80	μmol photons m^{-2} s^{-1}	Vasconcelos *et al.*, 2019
H_M	Half-saturation constant of light-dependent growth of mixoplankton	80	μmol photons m^{-2} s^{-1}	Same as an autotroph
I_0	PAR at lake surface	300	μmol photons m^{-2} s^{-1}	Approximate average summer irradiation averaged over a full daily cycle
J_{BM}	Maximum ingestion rate of bacteria by mixoplankton	3.0	d^{-1}	Menon *et al.*, 1996
J_{LB}	Maximum uptake rate of labile C by bacteria	6	d^{-1}	Yields a maximum C-limited bacterial growth rate of $c_{LB}*J_{LB} = 3$
J_{PB}	Maximum uptake rate of inorganic P by bacteria	0.11	g P g^{-1} C d^{-1}	Yields a maximum nutrient-limited bacterial growth rate of $q_T/q_B*J_{LB} + J_{PB}/q_B = 2.4$
k_A	Light attenuation coefficient of autotroph	0.3	m^2 C g^{-1}	Vasconcelos *et al.*, 2019
k_M	Light attenuation coefficient of mixoplankton	0.3	m^2 C g^{-1}	Same as an autotroph
k_T	Light attenuation coefficient of CDOM	0.2	m^2 C g^{-1}	Vasconcelos *et al.*, 2019
k_W	Light attenuation coefficient of clear water	0.02	m^{-1}	Hass and Davisson, 1977
l_A	Metabolic and mortality loss rate of autotroph	0.15	d^{-1}	Vasconcelos *et al.*, 2019
l_B	Metabolic and mortality loss rate of bacteria	0.25	d^{-1}	Personal communication
l_M	Metabolic and mortality loss rate of mixoplankton	0.15	d^{-1}	Same as an autotroph
p_A	Maximum light- and inorganic P-dependent growth rate of autotrophs	1.5	d^{-1}	Vasconcelos *et al.*, 2019
p_M	Maximum light- and inorganic P-dependent growth rate of mixoplankton	1.5	d^{-1}	Same as an autotroph
q_A	P to C quota of autotroph	0.012 0.025	g P g^{-1} C	Vasconcelos *et al.*, 2019 Le Noac'h MS
q_B	P to C quota of bacteria	0.05	g P g^{-1} C	Vrede, 1998

(continued)

Table II: *Continued*

Variables/ parameters	Definition	Value	Units	Source or justification
q_M	P to C quota of mixoplankton	0.025	g P g^{-1} C	Same as an autotroph
q_T	P to C quota in CDOM	0.00176	g P g^{-1} C	Vasconcelos *et al.*, 2019
P_{in}	Concentration of inorganic P in influx	0–0.2	g P m^{-3}	Possible range in nature
S_{BM}	Half-saturation constant of bacteria consumption by mixoplankton	0.25	g C m^{-3}	Menon *et al.*, 1996
S_{CB}	Half-saturation constant of uptake by bacteria	0.03	g C m^{-3}	Modified from Jansson *et al.*, 2006
S_{PA}	Half-saturation constant of inorganic P-dependent growth of autotrophs	0.003	g P m^{-3}	Vasconcelos *et al.*, 2019
S_{PB}	Half-saturation constant of inorganic P uptake by bacteria	0.0008	g P m^{-3}	Šimek *et al.*, 2006
S_{PM}	Half-saturation constant of inorganic P -dependent growth of mixoplankton	0.003	g P m^{-3}	Same as an autotroph
z_{max}	Depth of the mixed water column	7	m	Assumed

The last column lists empirical sources or explanations/justifications for the chosen values.

Simulation analyses

All model simulations were run to equilibrium; therefore, the initial conditions had no impact on reported model results. The specific period of time that each set of simulations was run for is reported below. Unless otherwise stated, the value of mixoplankton autotrophic investment (α) was set to 0.5, representing equal effort invested in the acquisition of resources through predation of bacteria versus autotrophy, as previously described. A maximum water column depth (z_{max}) of 7 m was used for all reported simulations. To check the robustness of results against changes in water column depth, we also ran analyses with z_{max} set to 3 m. The resulting trends were qualitatively similar and are therefore not reported.

To illustrate transient system dynamics, as well as the stabilizing influence of CDOM supply (C_{Tin}) and mixoplankton (M) presence on the interaction between autotrophs (A) and bacteria (B), we first show single time series simulations that were run under low phosphorous supply ($P_{in} = 0.025$ g P m^{-3}) and with four different model structures. The model structures are (i) M absent and C_{Tin} at zero, (ii) M absent and C_{Tin} at 50 g C m^{-3}, (iii) M present and C_{Tin} at zero and (iv) M present and C_{Tin} at 50 g C m^{-3}. We report model dynamics through simulated day 1000.

Using the full model with all state variables present, we subsequently explore equilibrium conditions across CDOM and phosphorous supply gradients, generating bifurcation plots for visual analysis. Supply gradients were accomplished by varying the incoming concentrations of CDOM and mineral phosphorus from 0 to 120 g C m^{-3} and from 0 to 0.2 g P m^{-3}, respectively. Both gradient ranges were broken into 201 increments that, when crossed, yielded a total of 40 401 different CDOM and phosphorous supply conditions used for simulations. The densities, concentrations and states reported in these plots were taken from the simulated day on which equilibrium was reached (defined as the point when the Euclidian norm of the solution vector was <1e-8). Plots were generated for all state variables and for the growth limiting resource of each biotic population. Additional plots show the fractional contribution of bacteria to the phosphorous and carbon assimilated by mixoplankton.

To better understand the effect of autotrophic investment (α) on mixoplankton abundance, we ran simulations across the previously described resource gradient but using either decreased (0.2) or increased (0.8) values of α (default value = 0.5). We generated bifurcation plots to visualize mixoplankton biomass, resource limitation and the contribution of resources obtained from bacteria to mixoplankton growth.

RESULTS

Effects of mixoplankton and CDOM on the stability of system dynamics

Under relatively low nutrient supply ($P_{in} = 0.025$ g P m^{-3}) and in absence of both a mixoplankton population and CDOM supply ($C_{Tin} = 0$), system dynamics are intrinsically unstable and shift between two states (Fig. 2a). In one state bacterial growth is suppressed by strong carbon limitation and bacteria, therefore, cannot control inorganic phosphorous. This allows autotrophs to sequester most of the system's phosphorous and subsequently become nutrient-limited and start releasing surplus photosynthate as labile carbon. This, in turn, relieves bacterial carbon limitation, allowing bacteria to gain control of inorganic phosphorous and deplete it to levels where autotrophs decline and stop excreting labile carbon. In this state, bacterial growth continues until the labile carbon stock is depleted and the population starts to decline, thus releasing control of the dissolved inorganic phosphorous pool and initiating the next cycle.

Introduction of mixoplankton (in absence of CDOM) strongly stabilizes system dynamics (Fig. 2b). Under this scenario, mixoplankton suppress the autotroph-bacteria cycles by controlling bacterial biomass at low levels through predation. Bacteria are then unable to reduce phosphorous to levels that would cause autotroph starvation, which, in turn, promotes a stable production of labile carbon that supports bacterial growth. The addition of CDOM (in absence of mixoplankton) also stabilizes the system, yet through a different mechanism

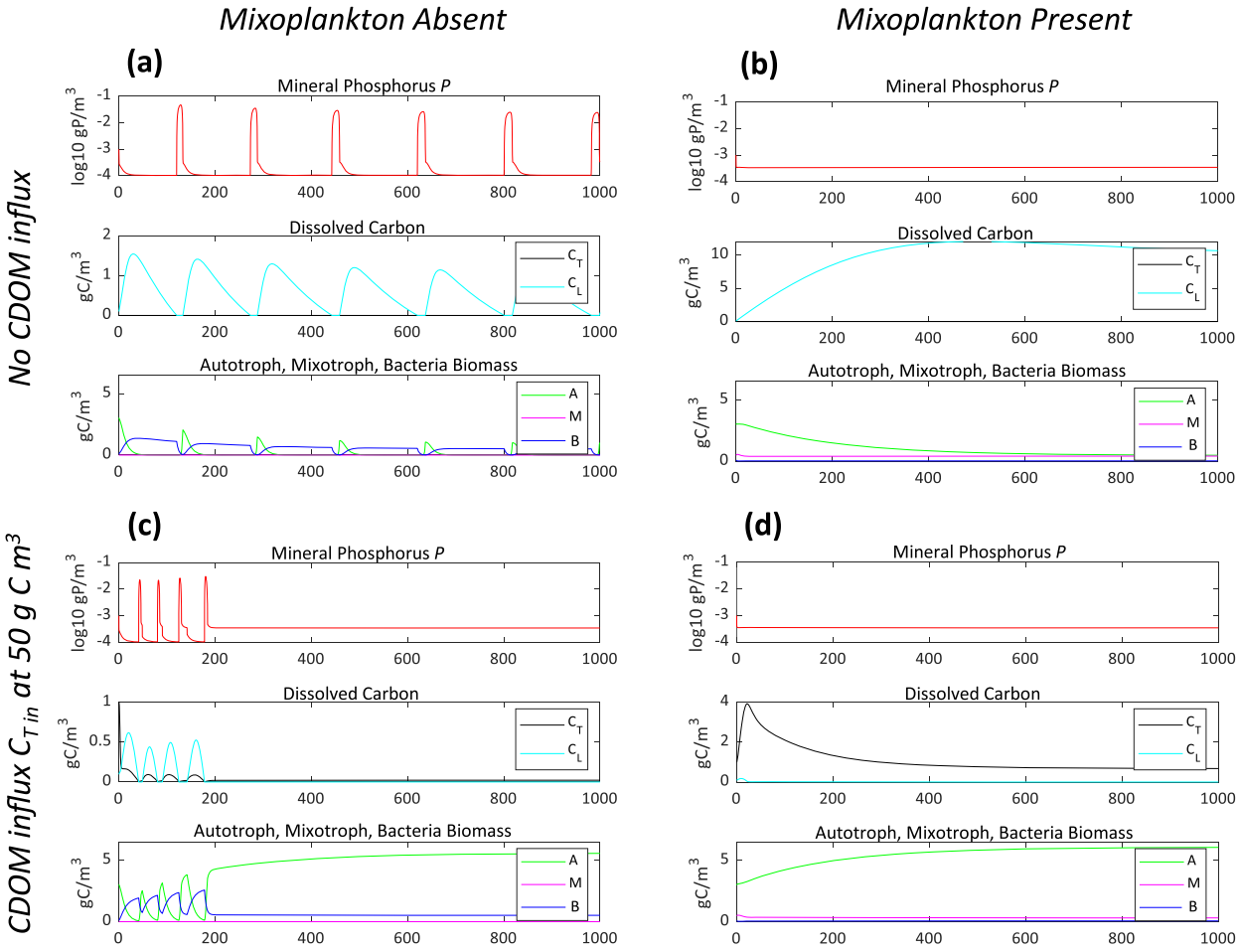

Fig. 2. Time series plots illustrating the stabilizing effect of mixoplankton (**b** & **d**) and terrestrial CDOM (**c** & **d**) on model dynamics, which are unstable under low nutrient supply ($P_{in} = 0.025$ g P m^{-3} for all simulations) when mixoplankton is absent and CDOM supply is at zero (**a**). CDOM supply is 50 g C m^{-3} in panels (c) and (d). Legends indicate line colors representing dissolved inorganic phosphorous (P), terrestrial CDOM (C_T), labile carbon (C_L), autotrophic phytoplankton (A), mixoplankton (M) and heterotrophic bacterioplankton (B). All y-axis scales are constant across panels (a–d) with the exception of the dissolved carbon panels.

(Fig. 2c). In this case, phosphorous originally bound to CDOM accumulates in the system during transient dynamics and releases autotroph phosphorous limitation in a two-step process: Added CDOM initially supplements bacterial growth, but is subsequently mineralized into the inorganic phosphorous pool via bacterial metabolism and mortality, most of which, after a series of transient oscillations, becomes sequestered in autotroph biomass. Equilibrium is reached when autotroph biomass becomes high enough to induce light limitation, thus bringing the production of labile carbon to an abrupt halt. Under these conditions, bacterial production becomes strongly carbon-limited (maintained exclusively by CDOM supply), which prevents bacteria from reducing mineral phosphorus to levels that would initiate further oscillations.

When both mixoplankton and CDOM are present in the system, the above two mechanisms combine to suppress transient oscillations (through mixotroph grazing of bacteria) and yield high, light-limiting levels of autotroph biomass (supported by phosphorus originating from CDOM) (Fig. 2d). Bacteria are kept at low densities by mixoplankton, and (energy limited) mixoplankton are kept at low densities by the combination of low bacterial prey density and strong shading from autotrophs. In conclusion, since mixoplankton and CDOM are present in nearly the entire CDOM and nutrient supply space that will be explored in subsequent sections, the system always reaches a stable point and we focus our analyses on the resulting equilibrium states.

Effect of CDOM and inorganic phosphorous on biotic state variables

When the full range of the CDOM supply gradient is considered, the following overarching response patterns to browning emerge (Fig. 3). If we disregard regions of no change (dotted areas in Fig. 3), light availability and labile carbon concentration both decrease (Fig. 3g, j) and bacterial biomass and mineral phosphorus concentration both increase (Fig. 3c and i) with increasing CDOM supply. In contrast, autotroph biomass is unimodally

related to CDOM supply, except at very high levels of mineral nutrient supply where autotroph biomass only decreases with browning (Fig. 3a). Finally, while CDOM concentration and mixoplankton both increase monotonically with browning when mineral phosphorus supply is very high, they show more complex responses to browning when mineral phosphorus supply is lower (Fig. 3b and h). Notably, for most levels of mineral nutrient supply, mixoplankton shows a U-shaped response to browning (Fig. 3b).

The three plankton populations thus show distinctly different responses to browning. These different responses are, however, intimately related and can be largely understood from knowledge of which resource type (energy vs. nutrient) limits population growth rates at a given combination of external CDOM and mineral phosphorus supply. If we ignore extreme scenarios where the supply of CDOM and mineral phosphorus is too low to allow persistence of all three plankton populations (region near the origin in Fig. 3a–c), the system will, with increasing CDOM supply, go through several distinct states that differ in terms of which plankton populations and resources increase, decrease or stay constant. We illustrate this with the default example where mixoplankton investment in photosynthesis is intermediate ($\alpha = 0.5$). We first focus on a transect of increasing CDOM supply at low mineral nutrient supply (scenario 1 in Figs 3d–f and 4) before we describe the patterns occurring at higher mineral nutrient supply (scenarios 2 and 3 in Figs 3d–f, 5 and S1). Analytical derivations supporting the generality of the predicted patterns are given in Appendix S1 with a summary provided in Table S1.

Scenario 1. At relatively low mineral phosphorus supply (scenario 1 in Fig. 3d–f), growth of all three plankton populations is phosphorus limited if CDOM supply is also low (below solid white lines in Fig. 3). Under these circumstances, stable coexistence of all three populations entails that both mineral phosphorus and bacteria are controlled at fixed levels by autotrophs and mixoplankton, respectively, because the nutrient-dependent specific growth rates of autotrophs and mixoplankton must balance their constant specific losses. Consequently, both mineral phosphorus concentration and bacterial biomass remain constant, whereas autotroph and mixoplankton biomass increase with increasing CDOM and, thus, increasing organic phosphorus supply (region below solid white lines in Fig. 3a–c, l; $C_{T\mathit{in}} < 10$ g C m^{-3} in Fig. 4a–d). While the additional organic phosphorus from CDOM is initially consumed by bacteria, it becomes ultimately sequestered in protist biomass. Increased protist biomass, in turn, increases light attenuation (Figs 3j and 4f) until a threshold CDOM input is reached, at which light availability becomes so low that the specific growth rate of mixoplankton becomes energy limited (Fig. 3e and solid lines in Fig. 3a–c and g–l; $C_{T\mathit{in}} > 10$ g C m^{-3} in Fig. 4i).

Mixoplankton become energy-limited at a much lower CDOM supply than autotrophs and bacteria (Figs 3d–f and 4g–i). This is due to half of their resource acquisition effort being geared toward bacterial predation, a good source of phosphorus (because of high bacterial P:C ratio) but a poor source of energy (because of low bacterial biomass and relatively low conversion efficiency). In the parameter region below the solid line in Fig. 3, where mixoplankton are phosphorous limited, ∼50% of their phosphorus but <20% of their energy comes from bacteria (Fig. 3k–l). Mixoplankton thus obtain >80% of their energy from photosynthesis but with a photosynthetic effort only half that of autotrophs. This, in turn, explains why autotrophs and bacteria become energy-limited at much higher levels of CDOM supply, where increased self-shading limits autotroph growth, shutting down the bacteria's labile carbon source as further described below.

Once energy is limited, mixoplankton can only persist in the system under increasing CDOM supply if their energy intake from the consumption of bacteria compensates for reduced photosynthesis. This requires a weakening of the control of bacterial biomass by mixoplankton. As long as autotroph and bacterial growth remain nutrient-limited, biomass of both, therefore, increase with CDOM (= organic phosphorus) input, whereas the energy-limited mixoplankton population decreases in most of this parameter region (area between solid and broken lines in Fig. 3a–c; $10 < C_{T\mathit{in}} < 74$ g C m^{-3} in Fig. 4a–c). The decrease in mixoplankton is a consequence of reduced photosynthesis (caused by increased shading from autotrophs, Figs 3j and 4f) that cannot be fully compensated by energy acquisition from bacteria (note that bacterial biomass is one order of magnitude lower than mixoplankton biomass). The increase in autotroph biomass and concomitant shading with increasing CDOM supply continues until a threshold is reached at which the specific growth rate of autotrophs becomes (light) energy limited (Fig. 3d and broken lines in Fig. 3a–c, g–l; $C_{T\mathit{in}} > 74$ g C m^{-3} in Fig. 4g).

From thereon (region between broken and dash-dotted lines in Fig. 3), no excess photosynthate is produced (labile carbon goes to zero, Fig. 3g), and autotrophs can only persist in the system if light availability does not change with further increases in CDOM input (dotted area in Fig. 3j; $74 < C_{T\mathit{in}} < 110$ g C m^{-3} in Fig. 4f) because the light-dependent specific growth rate of autotrophs must balance their constant specific losses. Constant light availability under increasing CDOM supply implies, in turn, constant bacterial biomass (mixoplankton control bacteria such that the energy intake from constant photosynthesis and constant ingestion of bacteria balances constant specific losses, Figs 3c and 4b) and concomitant increases in CDOM concentration (because constant bacterial biomass cannot consume all of the additional CDOM input, Figs 3h and 4e) and mixoplankton (because a higher CDOM concentration leads to higher specific bacterial growth, which must be balanced by higher bacterial predation from mixoplankton, Figs 3b and 4c). Finally, since higher CDOM supply leads to higher light attenuation from more mixoplankton and CDOM, the biomass of autotrophs must decrease to maintain a constant light environment (Figs 3a and 4a).

This decline in autotroph biomass continues up to a threshold in CDOM supply at which the autotroph population goes extinct (dash-dotted line in Fig. 3a; $C_{T\mathit{in}} > 110$ g C m^{-3} in Fig. 4a). From thereon, increased light attenuation from CDOM can no longer be compensated by decreased autotroph biomass. With increasing CDOM supply, light availability therefore declines (Figs 3j and 4f), bacterial biomass increases (fueled by more CDOM, Fig. 3c, Fig. 4b) and mixoplankton decrease slightly (because increased ingestion of bacteria cannot fully compensate for reduced photosynthesis, Figs 3b and 4c). In the hypothetical limit of infinite CDOM supply, bacteria and mixoplankton

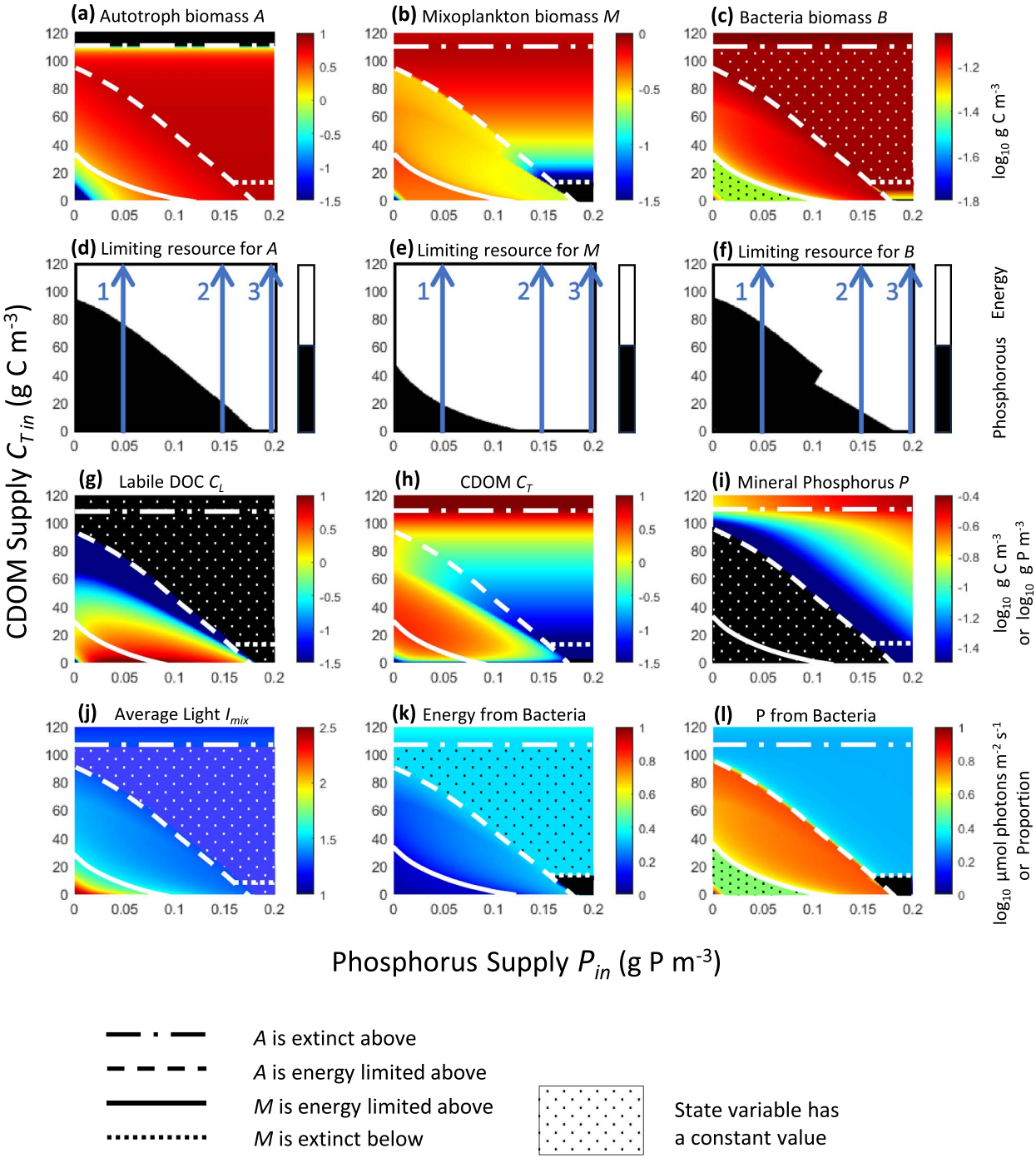

Fig. 3. Equilibrium values, states or proportions from model simulations run over a gradient of mineral phosphorous (P_{in}) and terrestrial CDOM (C_{Tin}) supply and with the mixoplankton investment in autotrophy (α) set at 0.5. Top panels show the biomasses of **(a)** autotrophic phytoplankton, **(b)** mixoplankton and **(c)** heterotrophic bacterioplankton, with black shading indicating population extinction. Second-row panels show the growth-limiting resource (energy or phosphorus, **d–f**) for each population, with numbered arrows indicating the phosphorous supply transects at 0.05, 0.15 and 0.19 g C m^{-3} shown in Figs 4, 5 and S1, respectively. Third-row panels show the ambient concentrations of **(g)** labile carbon, **(h)** terrestrial CDOM and **(i)** mineral phosphorous, with black shading indicating a concentration of zero in panel (g) and of 0.00035 g P m^{-3} in panel (i). Fourth-row panels show **(j)** the average photon flux density in the water column, **(k)** the proportion of energy that mixoplankton acquires from bacterial prey vs. photosynthetic fixation and **(l)** the proportion of phosphorous that mixoplankton acquires from prey vs. mineral phosphorous, with black shading indicating a proportion = 0. In all panels, dotted areas indicate that a variable is constant and white lines trace extinction boundaries or boundaries at which switches in the growth-limiting resource occur as indicated in the legend.

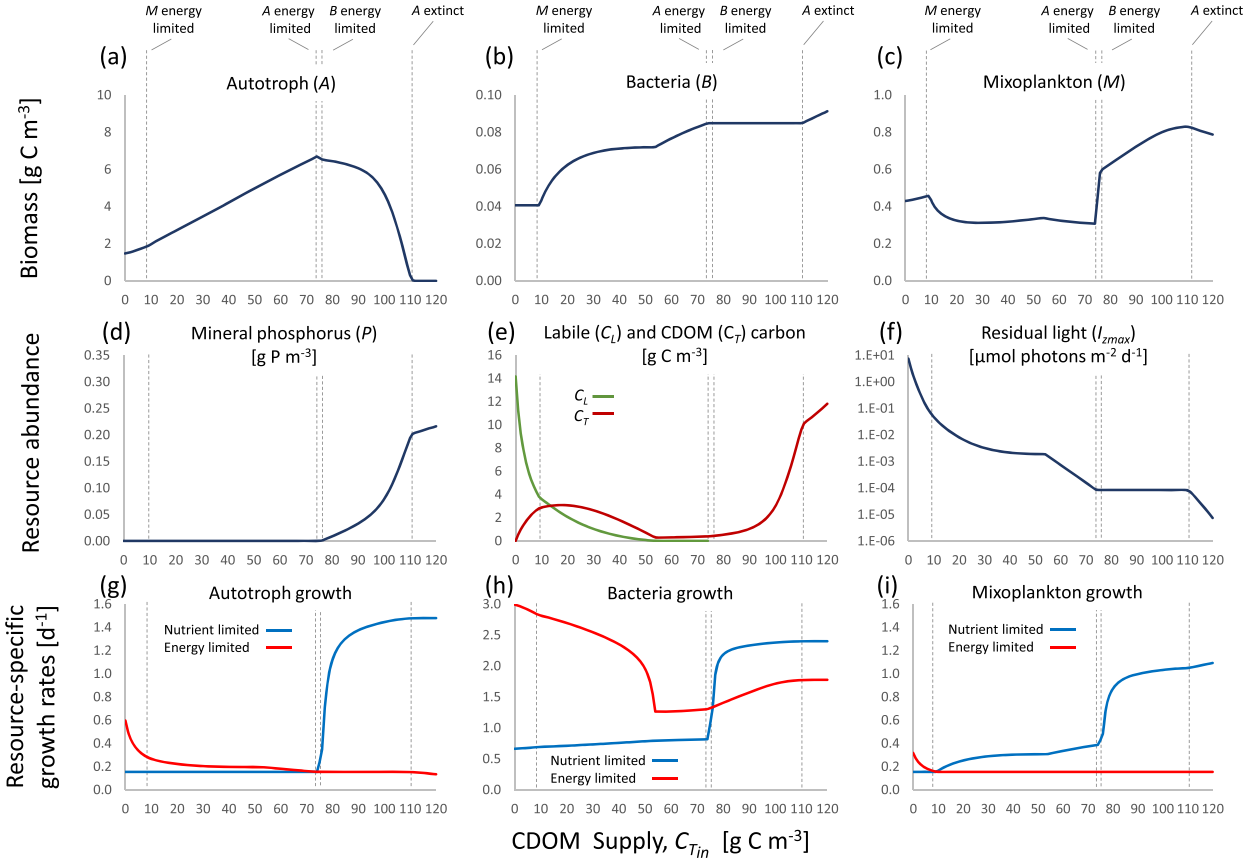

Fig. 4. Equilibrium values of population biomasses, resource abundances and resource-specific growth rates along a transect of increasing terrestrial CDOM supply at a phosphorous supply $P_{in} = 0.05$ g P m^{-3} (arrow 1 in Fig. 3). Dotted lines mark CDOM supply levels at which major transitions occur, including switches from phosphorus to energy limitation of mixoplankton (M), autotrophs (A), and bacteria (B) and the extinction of autotrophs.

will either reach asymptotic biomass levels (if mixoplankton can persist in near-complete darkness on bacteria alone) or mixoplankton will go extinct (if some level of photosynthesis is required for mixoplankton persistence).

Scenario 3. When mineral phosphorus supply is sufficiently high (scenario 3, $R_{in} > 0.18$ g P m^{-3} in Fig. 3d–f), all three plankton populations are already energy-limited in the complete absence of external CDOM. Under these conditions ($C_{Tin} = 0$, lower right corner in Fig. 3a–c, g), autotrophs suppress both bacteria and mixoplankton, because bacteria lack an energy source (no labile carbon is excreted when autotroph production is light-limited) and, consequently, mixoplankton cannot compensate their inferiority in competition for light by feeding on bacteria. Gradually increasing CDOM supply will then allow the establishment of a bacterial population that increases to a threshold beyond which a mixoplankton population can be sustained (dotted line in Fig. 3a–c; $C_{Tin} = 15$ g C m^{-3} in Fig. 5b–c). Once all three energy-limited populations can coexist, scenario 3 produces the same system responses to increasing CDOM supply as does scenario 1 under energy limitation (dotted area in Fig. 3c and j); i.e. autotroph biomass declines, light availability and bacterial biomass remain constant and CDOM, mineral phosphorus and mixoplankton increase (Fig. 3a–c, g–i; $15 < C_{Tin} < 110$ g C m^{-3} in Fig. 5).

Scenario 2. Finally, when mineral phosphorus supply is intermediate ($0.11 < R_{in} < 0.18$ g P m^{-3}, scenario 2 in Fig. 3d–f), only the growth of mixoplankton is energy limited in the absence of CDOM input ($C_{Tin} = 0$ in Fig. S1g–i). System responses to browning are then a continuation of scenario 1 in the lower range of CDOM supply, where growth of bacteria and autotrophs is still nutrient-limited, and scenario 3 in the upper range of CDOM supply, where all three populations are energy-limited. The transition between these response patterns is, however, discontinuous at the CDOM supply threshold where bacteria become energy-limited abruptly (Fig. S1h), producing a very narrow range of alternative states and a discontinuous dip in mixoplankton biomass that requires a considerable further increase in CDOM supply to be recovered (Figs 3b and S1c).

Effects of the mixoplankton's investment in autotrophy

Shifting the mixoplankton's investment in autotrophy away from the default value of $\alpha = 0.5$ has two main effects. First, lower investment in autotrophy (lower α) moves the boundary at which mixoplankton switches from phosphorus to energy limitation toward lower CDOM and phosphorus supply (Fig. 6c–d). This can again be explained by the fact that mixoplankton predation suppresses bacteria to very low densities, making them a scarce energy source but still a decent phosphorus source

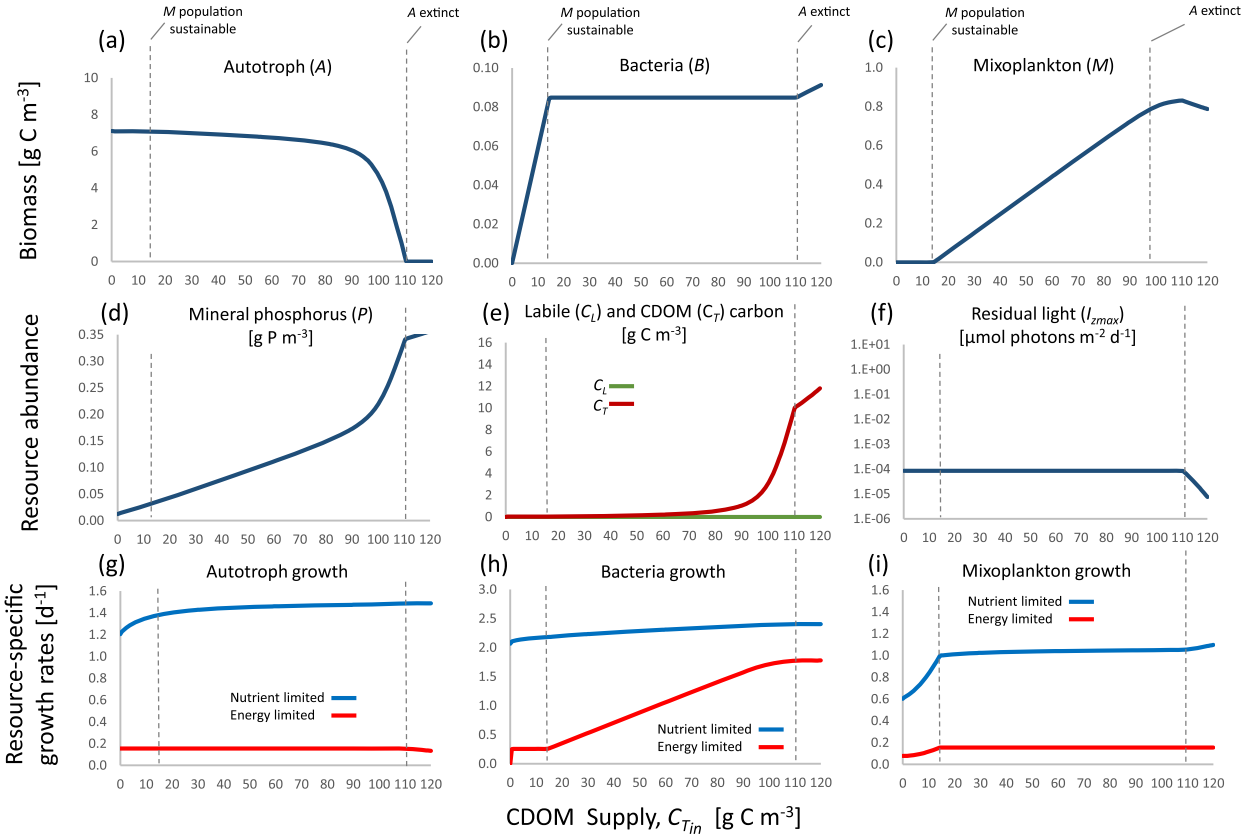

Fig. 5. Equilibrium values of population biomasses, resource abundances and resource-specific growth rates along a transect of increasing terrestrial CDOM supply at a phosphorous supply $P_{in} = 0.19$ g P m^{-3} (arrow 3 in Fig. 3). Dotted lines mark CDOM supply levels at which major transitions occur, including the sustained persistence of mixoplankton (M) and the effective extinction of autotrophs (A).

(because of the high bacterial P:C ratio). For example, in the region where mixoplankton is energy limited and autotrophs are phosphorus limited (between solid and broken lines in Fig. 6), mixoplankton with $\alpha = 0.2$ obtain >95% of their phosphorus but only 50–60% of their energy from bacteria (Fig. 6e and g). The latter cannot be compensated by the low photosynthetic effort, leading to a switch from phosphorus to energy limitation of mixoplankton at very low CDOM and phosphorus supplies (Fig. 6c). In contrast, mixoplankton with a high photosynthetic effort ($\alpha = 0.8$) become energy limited at similar CDOM-nutrient supply regimes as do autotrophs (Fig. 6d).

Second, higher investment in autotrophy (higher α) yields higher mixoplankton biomass over the entire CDOM-phosphorus supply space (Fig. 6a and b), and increases the contribution of mixoplankton to total protist biomass $M/(M+A)$ in the resource supply space where mixoplankton and autotrophs coexist (Fig. 7). Both observations suggest that, in our model, competition for (light) energy from autotrophs can strongly limit mixoplankton biomass. In contrast, the reverse competitive effect of mixoplankton on autotrophs is relatively weak, as indicated by two lines of evidence. First, higher mixoplankton biomass at higher α has only a weak negative effect on autotroph biomass (data not shown). Second, the mixoplankton's autotrophic investment has an almost negligible effect on where autotrophs switch from nutrient to energy limitation in the CDOM-phosphorus supply space (broken lines in Fig. 6). The latter implies that the CDOM-phosphorus supply region in which mixoplankton shows a primarily negative to neutral response to increasing CDOM supply (region between solid and broken lines in Figs 3b and 6a–b) is largest when mixotrophic investment in autotrophy is smallest. While the exact size and shape of this region depend on details of the protists' traits (as expressed in model parameters), we can generally conclude that mixoplankton performs comparatively poorly under CDOM-phosphorus supply regimes where its growth is energy-limited while the growth of autotrophs is phosphorus limited.

DISCUSSION

Mixoplankton nutritional strategies

By varying the mixoplankton's investment into photosynthesis α, we could explore mixoplankton nutritional strategies that are more-or-less reliant on autotrophic resources (inorganic phosphorous and light) versus heterotrophic resources (prey carbon and phosphorus). This yielded a very clear, overarching result: owing to both the low abundance and the low carbon-to-phosphorous ratio of bacteria, mixoplankton becomes more easily energy limited (Fig. 6c) and overall less competitive when its foraging effort on bacterial prey is increased at the expense of photosynthetic investment (Figs 3b and 6a and b). These results suggest that a strong investment in carbon acquisition through

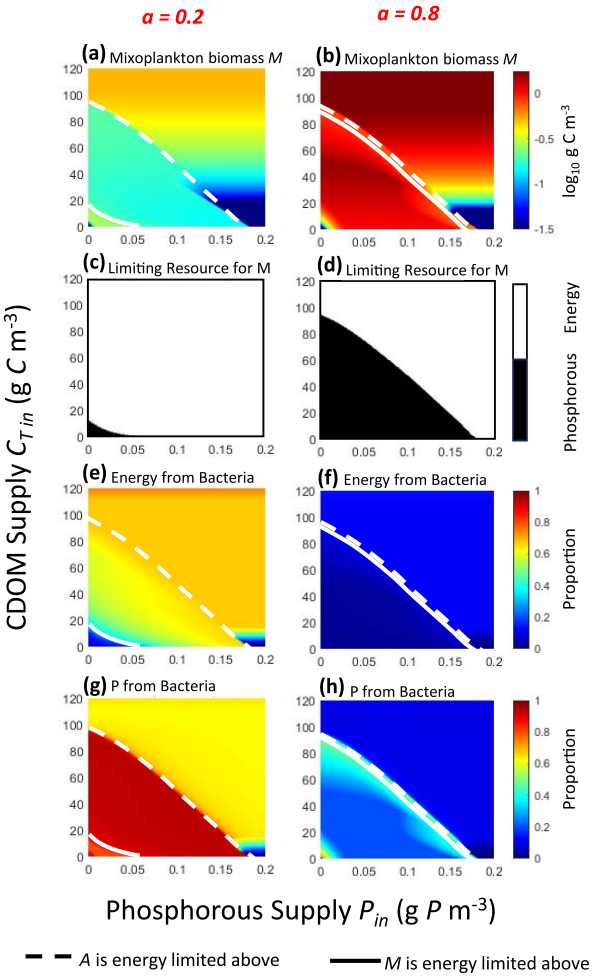

Fig. 6. Equilibrium values, states or proportions from model simulations run over a gradient of mineral phosphorous (P_{in}) and terrestrial CDOM (C_{Tin}) supply and with the mixoplankton investment in autotrophy (α) set at 0.2 (left column of panels) and 0.8 (right column of panels). Shown are **(a, b)** mixoplankton biomass, **(c, d)** the growth limiting resource of mixoplankton, **(e, f)** the proportion of energy that mixoplankton acquires from bacterial prey vs. photosynthetic fixation and **(g, h)** the proportion of phosphorous that mixoplankton acquires from prey vs. mineral phosphorous.

bacterivory is not ideal in most environments and support empirical work showing bacterivorous mixoplankton to be most competitive under high light, low nutrient conditions, where they obtain carbon through photosynthesis and nutrients from prey (Ptacnik *et al.*, 2016; Fischer *et al.*, 2017). The latter is exactly the CDOM and nutrient supply conditions under which our model predicts mixoplankton to dominate protist biomass (region near origin in Fig. 7). Such synergistic relationships, where the coupling of photosynthesis with phagotrophy allows for elevated growth, have been demonstrated as important to mixoplankton competitive fitness (Flynn and Mitra, 2023; Mitra and Flynn, 2023).

Our model results also suggest that phosphorous from bacterial prey is important for mixoplankton growth regardless of the autotrophic investment value. This is evidenced by the elevated proportion of phosphorous acquired by mixoplankton from bacterial prey to sustain growth under conditions where autotrophs are limited by inorganic phosphorous (region below the dashed white line in Figs 3l and 6g and h). Though poor mixotroph performance in this region is ultimately due to energy limitation, bacterial phosphorous is important for meeting the necessary quota to sustain the population's energy-limited growth. For example, mixoplankton obtain ~65–75% of their phosphorous from bacteria in the region where autotrophs are phosphorous limited (region below the dashed white line in Fig. 3i). If not for the acquired bacterial phosphorous, mixotrophs would likely not meet the P quota necessary to sustain energy-limited growth. This is in line with empirical studies demonstrating that phosphorous acquired from prey is important for mixoplankton growth or survival, especially under conditions of inorganic phosphorous scarcity (Caron *et al.*, 1993; Nygaard and Tobiesen, 1993; Flöder *et al.*, 2006). Had our model allowed for decoupling of the carbon and phosphorous autotrophic investment, such that it could be high for energy acquisition but low for phosphorous acquisition, mixoplankton phosphorous limitation might have been minimized through bacterivory, while simultaneous high levels of photosynthesis minimized energy limitation. In such a case, we suspect results may have shown higher mixoplankton biomass than was achieved.

Under the range of conditions tested, our results support mechanisms suggesting the most advantageous bacterivorous mixoplankton nutritional strategy to be one where carbon/energy is acquired through photosynthesis and phosphorous through predation. Further supporting these conclusions, physiological mixoplankton modeling work by Mitra and Flynn (2023) and Flynn and Mitra (2023) demonstrated that prey carbon was less important than prey phosphorous for mixoplankton growth under light saturating conditions. Such intersections between results from different modeling approaches are important as they point toward what are likely robust and generalizable system processes. It should be noted that different from our conceptual model, the detailed physiological model incorporates both photoacclimation processes and variable internal stoichiometry into mixoplankton growth determinations. Consideration of these processes in the context of an ecological model is certainly merited as they would alter the growth determinations of both protist groups (autotrophs and mixoplankton). We discuss these further below.

Influence of browning and eutrophication on network interactions

The model generates patterns along a large gradient in CDOM loading, which are broadly in line with empirical observations. To provide context for our model predictions, natural aquatic systems are considered "brown" when total organic carbon reaches 10 g m^{-3} (Blanchet *et al.*, 2022); however, lakes have been reported to reach levels near 50 g m^{-3} (Kritzberg *et al.*, 2020). Within the CDOM supply range investigated in our model system, ambient CDOM concentration reaches a high of 11.8 g m^{-3} under the highest level of CDOM loading (120 g m^{-3}). Interestingly, under low to intermediate (but not under high) mineral phosphorus supply, the model predicts

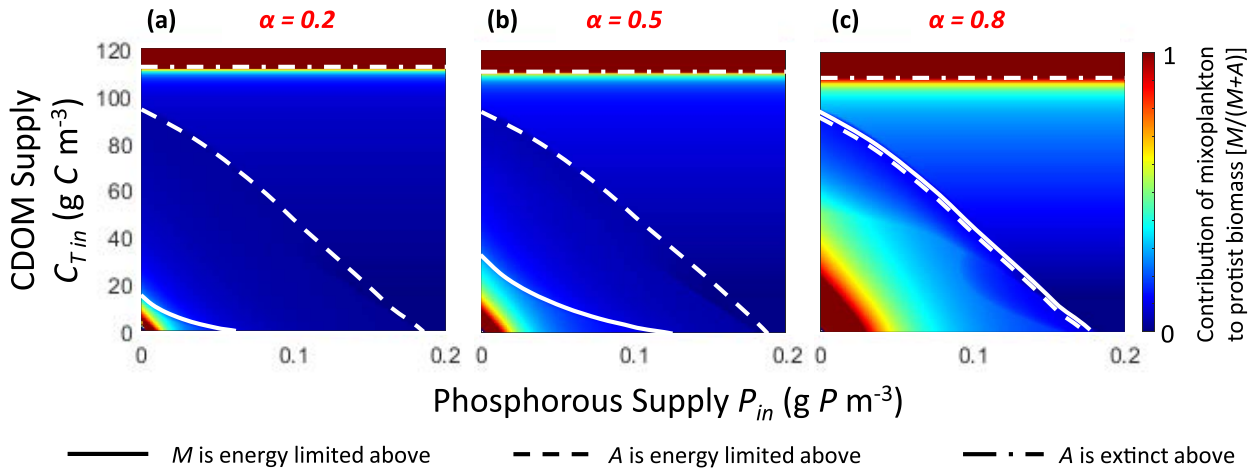

Fig. 7. The equilibrium contribution of mixoplankton to total protist biomass ($A+M/M$) over a gradient of mineral phosphorous (P_{in}) and terrestrial CDOM (C_{Tin}) supply, with the mixoplankton's investment in autotrophy set at **(a)** 0.2, **(b)** 0.5 and **(c)** 0.8.

a highly nonlinear, non-monotonous relationship between CDOM loading and ambient CDOM concentrations (Fig. 3h). This complex relationship is generated by variation in bacterial degradation of CDOM under different carbon and phosphorous supply conditions. Specifically, when both CDOM and mineral phosphorus supply are low to intermediate, bacterial growth is primarily supported by labile carbon that was excreted by phosphorus-limited autotrophs (Fig. 3g), leading to the accumulation of elevated concentrations of more recalcitrant CDOM. In contrast, under conditions of higher CDOM and/or higher phosphorus supply, the combination of elevated bacterial biomass (Fig. 3c) and a strongly reduced availability of labile carbon forces bacteria to rely on CDOM as their primary energy source, leading to increased bacterial degradation and relatively low ambient CDOM concentrations. Supporting the processes described here, work by Kritzberg *et al.* (2006) in experimental lake systems has shown that under conditions of low productivity and elevated CDOM, bacterial biomass is increasingly supported by allochthonous carbon over autochthonous sources and Kragh *et al.* (2008) demonstrated the potential for increased bacterial degradation of humic DOC with increasing phosphorous supply.

Several other model-generated patterns along the gradient of increasing CDOM supply are in agreement with empirical observations, including decreased light, increased inorganic phosphorous and bacteria and a shift to mixoplankton dominance of protist biomass under high CDOM supply. Thus, Tranvik (1988) observed in south Swedish lakes that bacterial biomass increased over a DOC range of 5–30 g m^{-3}. Whole-lake experiments in Wisconsin demonstrated that increased CDOM (over the range ~4–17 g m^{-3}) could reduce light (Carpenter *et al.*, 1998) and Ask *et al.* (2009) demonstrated a trend of decreasing light penetration with increasing allochthonous DOC in northern Swedish lakes. In temperate Canadian lakes, Senar *et al.* (2021) found that elevated terrestrial CDOM in the range of 8–12 g m^{-3} was associated with reductions in light, increased nutrients and a transition from autotroph to mixoplankton dominance. At similar ambient CDOM concentrations ~10 g m^{-3} (occurring near a loading concentration of 110 g m^{-3}), our model results show the decline of autotrophs and a concomitant shift to mixoplankton dominance.

Also, in qualitative agreement with empirical observations, as well as with earlier theoretical work (Kelly *et al.*, 2018; Vasconcelos *et al.*, 2018), our model predicts a unimodal relationship between CDOM loading and autotroph biomass, except under high phosphorous supply where the response is strictly negative. In northern Swedish lakes, Bergström and Karlsson (2019) indeed observed a unimodal relationship between phytoplankton biomass and CDOM concentration, with a peak in biomass near 11 g m^{-3} of DOC. While our work predicts peak biomass at much lower ambient CDOM concentrations, there are multiple potential explanations for this incongruency. The study of Swedish lakes considers all Chl*a*-containing biomass, including mixoplankton, which may compensate for pure autotrophs under low light conditions. In addition, we do not consider photo-acclimation processes, which may lead to underestimation of phytoplankton biomass in the model under low light conditions. Bergström and Karlsson (2019) also demonstrated that the occurrence of the unimodal relationship they observed was dependent on trophic status, whereas, in lakes with eutrophic conditions and high phytoplankton biomass, CDOM loading had only a negative impact, as light availability was the main control on growth such that addition of organic nutrients from CDOM did not increase biomass. Such findings further the notion that nutrient limitation is a prerequisite for positive CDOM supply effects on phytoplankton biomass and the potential for a unimodal relationship to occur. We note that model patterns between ambient CDOM concentrations and phytoplankton biomass were more complex than simple linear or unimodal relationships in many cases, but still support the potential for observation of a unimodal relationship in natural systems sampled across multiple resource gradients.

Over the full range of CDOM loading we found the mixoplankton response complex and dependent on multiple factors. The striking occurrence of a local mixoplankton minimum along the CDOM loading gradient is the result of interactions between

multiple network components, with underlying mechanisms that depend on phosphorus supply. At low phosphorus supply, the onset of a decline in mixoplankton occurs at the CDOM supply level where mixoplankton become energy-limited and start to suffer from increased shading by autotrophs (Fig. 4c). In contrast, at intermediate phosphorus supply, mixoplankton are energy-limited over the entire CDOM gradient but experience a discontinuous drop at the CDOM supply level where labile carbon production becomes negligible and bacterial production becomes abruptly and strongly energy-limited, and therefore cannot sustain a larger mixoplankton population (Fig. S1c). Under both of these phosphorus supply regimes, as the CDOM supply is further increased, the mixoplankton population begins to recover due to decreased shading from autotrophs and increased bacterial production with a new but less desirable carbon source. These biomass patterns, defined by an approximate "U" shape over the CDOM supply gradient, have, to our knowledge, not been reported in previous modeling or empirical studies. Indirect evidence that this pattern may indeed occur in natural systems comes from an empirical study of boreal Canadian lakes, where mixoplankton biomass was reported to show a "U" shaped relationship with CO_2 (Hansson *et al.*, 2019). In these same systems, CO_2 was reported to be highly correlated with CDOM.

Considering mixotroph biomass patterns across the phosphorous supply gradient, the model generally predicts mixoplankton biomass to decrease or hold constant as the system is eutrophied. In an analysis of data from 1652 North American lakes, Le Noac'h *et al.* (2024) identified lake trophic state as the primary indicator of mixoplankton (bacterivores and others) abundance. Here, light was found to be a relatively weak predictor of mixoplankton abundance. Our theoretical study supports these results, as model predictions show a complex relationship between light and mixoplankton abundance, where the effect of light depends on factors driving its availability. When light limitation is caused by elevated autotroph biomass due to enrichment, mixoplankton abundance is low, but when light limitation is caused by CDOM, mixoplankton are able to dominate the system. Such complexities likely contribute to the low predictive power of light for mixoplankton abundance across large environmental gradients in natural systems.

In creating a general and tractable ecosystem model, our framework was limited and some aspects of cellular physiology, including photoacclimation and variable stoichiometry, were not considered. From empirical work, we know that the stoichiometry of phytoplankton can fluctuate widely to accommodate processes such as luxury uptake of resources, storage of photosynthetic products and changes in Chl*a* content (Sterner and Elser, 2002). Such cellular mechanisms are important factors for autotrophic biomass accumulation. In addition, we do not consider crustacean or micro-zooplankton grazers in the network presented here. These organisms can potentially exert strong top-down control on phytoplankton biomass (Sommer *et al.*, 1986; Carpenter *et al.*, 2001; Sommer *et al.*, 2012) and introduce additional complexity to trophic network interactions (Ptacnik *et al.*, 2004). How each of these factors might influence model processes is difficult to deduce, given the complexity that arises under our current framework. Their consideration, including how they may differ between phytoplankton and mixoplankton organisms, are interesting avenues for future exploration.

CONCLUSION

Simulations along a dual CDOM and inorganic phosphorous supply gradient revealed predictable changes in the abundances of the different plankton populations and their resources. Model-produced patterns along the CDOM supply gradient that are in general agreement with empirical observations include increased bacterial biomass inorganic phosphorous with CDOM supply, decreased light penetration with elevated CDOM and potential for a unimodal phytoplankton biomass response. Results presented here also demonstrate the complex relationships underlying these responses and the usefulness of theoretical systems for dissection of complex network processes. Further, our findings provide insight into mechanisms that may underlie success of different mixoplankton life history strategies observed in nature across environmental gradients of browning and eutrophication, which reinforce the important role mixoplankton play creating a bridge or "shortcut" (Ptacnik *et al.*, 2016) between bacterial production and autotrophic primary production. Continued efforts to better understand impacts of phago-mixotrophy among the plankton are important given the ability of these organisms to increase trophic linkages and generate complex system feedbacks, especially in the face of continued anthropogenic and climate change related disturbances.

SUPPLEMENTARY DATA

Supplementary data can be found at *Journal of Plankton Research* online.

AUTHOR CONTRIBUTIONS

Sierra Cagle: Conceptualization, Methodology, Formal analysis, Writing—Original Draft.

Sebastian Diehl: Conceptualization, Methodology, Formal analysis, Writing—Review & Editing.

FUNDING

This work was funded in part by the ASLO Limnology and Oceanography Research Exchange Program (National Science Foundation award #1831075).

REFERENCES

Ask, J., Karlsson, J., Persson, L., Ask, P., Byström, P. and Jansson, M. (2009) Terrestrial organic matter and light penetration: effects on bacterial and primary production in lakes. *Limnol. Oceanogr.*, **54**, 2034–2040. https://doi.org/10.4319/lo.2009.54.6.2034.

Baines, S. B. and Pace, M. L. (1991) The production of dissolved organic matter by phytoplankton and its importance to bacteria: patterns across marine and freshwater systems. *Limnol. Oceanogr.*, **36**, 1078–1090. https://doi.org/10.4319/lo.1991.36.6.1078.

Bergström, A. K. and Karlsson, J. (2019) Light and nutrient control phytoplankton biomass responses to global change in northern lakes. *Glob. Chang. Biol.*, **25**, 2021–2029. https://doi.org/10.1111/gcb.14623.

Blanchet, C. C., Arzel, C., Davranche, A., Kahilainen, K. K., Secondi, J., Taipale, S., Lindberg, H., Loehr, J. *et al.* (2022) Ecology and extent of freshwater browning-what we know and what should be studied

next in the context of global change. *Sci. Total Environ.*, **812**, 152420. https://doi.org/10.1016/j.scitotenv.2021.152420.

Caron, D. A., Sanders, R. W., Lim, E. L., Marrasé, C., Amaral, L. A., Whitney, S., Aoki, R. B. and Porters, K. G. (1993) Light-dependent phagotrophy in the freshwater mixotrophic chrysophyte Dinobryon cylindricum. *Microb. Ecol.*, **25**, 93–111. https://doi.org/10.1007/BF00182132.

Carpenter, S. R., Cole, J. J., Hodgson, J. R., Kitchell, J. F., Pace, M. L., Bade, D., Cottingham, K. L., Essington, T. E. *et al.* (2001) Trophic cascades, nutrients, and lake productivity: whole-lake experiments. *Ecol. Monogr.*, **71**, 163–186. https://doi.org/10.1890/0012-9615(2001)071[0163:TCNALP]2.0.CO;2.

Carpenter, S. R., Cole, J. J., Kitchell, J. F. and Pace, M. L. (1998) Impact of dissolved organic carbon, phosphorus, and grazing on phytoplankton biomass and production in experimental lakes. *Limnol. Oceanogr.*, **43**, 73–80. https://doi.org/10.4319/lo.1998.43.1.0073.

Cotner, J. B. and Biddanda, B. A. (2002) Small players, large role: microbial influence on biogeochemical processes in pelagic aquatic ecosystems. *Ecosystems*, **5**, 105–121. https://doi.org/10.1007/s10021-001-0059-3.

Fischer, R., Giebel, H. A., Hillebrand, H. and Ptacnik, R. (2017) Importance of mixotrophic bacterivory can be predicted by light and loss rates. *Oikos*, **126**, 713–722. https://doi.org/10.1111/oik.03539.

Flöder, S., Hansen, T. and Ptacnik, R. (2006) Energy–dependent bacterivory in Ochromonas minima–a strategy promoting the use of substitutable resources and survival at insufficient light supply. *Protist*, **157**, 291–302. https://doi.org/10.1016/j.protis.2006.05.002.

Flynn, K. J. and Mitra, A. (2023) Feeding in mixoplankton enhances phototrophy increasing the potential for coastal water bloom-induced pH changes with ocean acidification. *J. Plankton Res.*, **45**, 636–651. https://doi.org/10.1093/plankt/fbad030.

Flynn, K. J., Stoecker, D. K., Mitra, A., Raven, J. A., Glibert, P. M., Hansen, P. J., Graneli, E. and Burkholder, J. M. (2013) Misuse of the phytoplanktonzooplankton dichotomy: the need to assign organisms as mixotrophs within plankton functional types. *J. Plankton Res.*, **35**, 3–11. https://doi.org/10.1093/plankt/fbs062.

Ghyoot, C., Flynn, K. J., Mitra, A., Lancelot, C. and Gypens, N. (2017) Modeling plankton mixotrophy: a mechanistic model consistent with the Shuter-type biochemical approach. *Front. Ecol. Evol.*, **5**, 78. https://doi.org/10.3389/fevo.2017.00078.

Hansson, T. H., Grossart, H. P., del Giorgio, P. A., St-Gelais, N. F. and Beisner, B. E. (2019) Environmental drivers of mixotrophs in boreal lakes. *Limnol. Oceanogr.*, **64**, 1688–1705. https://doi.org/10.1002/lno.11144.

Hass, M. and Davisson, J. W. (1977) Absorption coefficient of pure water at 488 and 541.5 nm by adiabatic laser calorimetry. *J. Opt. Soc. Am.*, **67**, 622–624.

Jansson, M., Bergström, A. K., Blomqvist, P. and Drakare, S. (2000) Allochthonous organic carbon and phytoplankton/bacterioplankton production relationships in lakes. *Ecology*, **81**, 3250–3255. https://doi.org/10.1890/0012-9658(2000)081[3250:AOCAPB]2.0.CO;2.

Jansson, M., Bergström, A. K., Lymer, D., Vrede, K. and Karlsson, J. (2006) Bacterioplankton growth and nutrient use efficiencies under variable organic carbon and inorganic phosphorus ratios. *Microb. Ecol.*, **52**, 358–364.

Joint, I., Henriksen, P., Fonnes, G. A., Bourne, D., Thingstad, T. F. and Riemann, B. (2002) Competition for inorganic nutrients between phytoplankton and bacterioplankton in nutrient manipulated mesocosms. *Aquat. Microb. Ecol.*, **29**, 145–159. https://doi.org/10.3354/ame029145.

Jones, R. I. (1998) Phytoplankton, primary production and nutrient cycling. In Tranvik, H. (ed.), *Aquatic Humic Substances: Ecology and Biogeochemistry*, Springer Berlin Heidelberg, Berlin, Heidelberg, pp. 145–175.

Karlsson, J., Bergström, A. K., Byström, P., Gudasz, C., Rodríguez, P. and Hein, C. (2015) Terrestrial organic matter input suppresses biomass production in lake ecosystems. *Ecology*, **96**, 2870–2876. https://doi.org/10.1890/15-0515.1.

Kelly, P. T., Solomon, C. T., Zwart, J. A. and Jones, S. E. (2018) A framework for understanding variation in pelagic gross primary production of lake ecosystems. *Ecosystems*, **21**, 1364–1376. https://doi.org/10.1007/s10021-018-0226-4.

Klug, J. L. (2005) Bacterial response to dissolved organic matter affects resource availability for algae. *Can. J. Fish. Aquat. Sci.*, **62**, 472–481. https://doi.org/10.1139/f04-229.

Kragh, T., Søndergaard, M. and Tranvik, L. (2008) Effect of exposure to sunlight and phosphorus-limitation on bacterial degradation of coloured dissolved organic matter (CDOM) in freshwater. *FEMS Microbiol. Ecol.*, **64**, 230–239. https://doi.org/10.1111/j.1574-6941.2008.00449.x.

Kritzberg, E. S., Cole, J. J., Pace, M. M. and Granéli, W. (2006) Bacterial growth on allochthonous carbon in humic and nutrient-enriched lakes: results from whole-lake 13 C addition experiments. *Ecosystems*, **9**, 489–499. https://doi.org/10.1007/s10021-005-0115-5.

Kritzberg, E. S., Hasselquist, E. M., Škerlep, M., Löfgren, S., Olsson, O., Stadmark, J., Valinia, S., Hansson, L. *et al.* (2020) Browning of freshwaters: consequences to ecosystem services, underlying drivers, and potential mitigation measures. *Ambio*, **49**, 375–390. https://doi.org/10.1007/s13280-019-01227-5.

Le Noac'h, P., Cremella, B., Kim, J., Soria-Píriz, S., del Giorgio, P. A., Pollard, A. I., Huot, Y. and Beisner, B. E. (2024) Nutrient availability is the main driver of nanophytoplankton phago-mixotrophy in North American lake surface waters. *J. Plankton Res.*, **46**, 9–24. https://doi.org/10.1093/plankt/fbad054.

Le Noac'h, P., Diehl, S. and Beisner, B. E. (2025) Vertical niche partitioning and the performance of mixotrophic generalists against autotrophic and heterotrophic specialists under contrasting light-nutrient supply regimes. *Am. Nat.*, in press.

Menon, P., Becquevort, S., Billen, G. and Servais, P. (1996) Kinetics of flagellate grazing in the presence of two types of bacterial prey. *Microb. Ecol.*, **31**, 89–101.

Mitra, A. and Flynn, K. J. (2023) Low rates of bacterivory enhances phototrophy and competitive advantage for mixoplankton growing in oligotrophic waters. *Sci. Rep.*, **13**, 6900. https://doi.org/10.1038/s41598-023-33962-x.

Mitra, A., Flynn, K. J., Burkholder, J. M., Berge, T., Calbet, A., Raven, J. A., Graneli, E., Glibert, P. M. *et al.* (2014) The role of mixotrophic protists in the biological carbon pump. *Biogeosciences*, **11**, 995–1005. https://doi.org/10.5194/bg-11-995-2014.

Monod, J. (1949) The growth of bacterial cultures. *Ann. Rev. Microbiol.*, **3**, 371–394. https://doi.org/10.1146/annurev.mi.03.100149.002103.

Mustaffa, N. I. H., Kallajoki, L., Biederbick, J., Binder, F. I., Schlenker, A. and Striebel, M. (2020) Coastal ocean darkening effects via terrigenous DOM addition on plankton: an indoor mesocosm experiment. *Front. Mar. Sci.*, **7**, 547829. https://doi.org/10.3389/fmars.2020.547829.

Nygaard, K. and Tobiesen, A. (1993) Bacterivory in algae: a survival strategy during nutrient limitation. *Limnol. Oceanogr.*, **38**, 273–279. https://doi.org/10.4319/lo.1993.38.2.0273.

Princiotta, S. D., Smith, B. T. and Sanders, R. W. (2016) Temperature-dependent phagotrophy and phototrophy in a mixotrophic chrysophyte. *J. Phycol.*, **52**, 432–440. https://doi.org/10.1111/jpy.12405.

Ptacnik, R., Gomes, A., Royer, S. J., Berger, S. A., Calbet, A., Nejstgaard, J. C., Gasol, J. M., Isari, S. *et al.* (2016) A light-induced shortcut in the planktonic microbial loop. *Sci. Rep.*, **6**, 29286. https://doi.org/10.1038/srep29286.

Ptacnik, R., Sommer, U., Hansen, T. and Martens, V. (2004) Effects of microzooplankton and mixotrophy in an experimental planktonic food web. *Limnol. Oceanogr.*, **49**, 1435–1445. https://doi.org/10.4319/lo.2004.49.4_part_2.1435.

Räike, A., Taskinen, A., Härkönen, L. H., Kortelainen, P. and Lepistö, A. (2024) Browning from headwaters to coastal areas in the boreal region: trends and drivers. *Sci. Total Environ.*, **927**, 171959. https://doi.org/10.1016/j.scitotenv.2024.171959.

Schmidtke, A., Bell, E. M. and Weithoff, G. (2006) Potential grazing impact of the mixotrophic flagellate Ochromonas sp.

(Chrysophyceae) on bacteria in an extremely acidic lake. *J. Plankton Res.*, **28**, 991–1001. https://doi.org/10.1093/plankt/fbl034.

Seekell, D. A., Lapierre, J. F., Ask, J., Bergström, A. K., Deininger, A., Rodríguez, P. and Karlsson, J. (2015a) The influence of dissolved organic carbon on primary production in northern lakes. *Limnol. Oceanogr.*, **60**, 1276–1285. https://doi.org/10.1002/lno.10096.

Seekell, D. A., Lapierre, J. F. and Karlsson, J. (2015b) Trade-offs between light and nutrient availability across gradients of dissolved organic carbon concentration in Swedish lakes: implications for patterns in primary production. *Can. J. Fish. Aquat. Sci.*, **72**, 1663–1671. https://doi.org/10.1139/cjfas-2015-0187.

Selosse, M. A., Charpin, M. and Not, F. (2017) Mixotrophy everywhere on land and in water: the grand écart hypothesis. *Ecol. Lett.*, **20**, 246–263. https://doi.org/10.1111/ele.12714.

Senar, O. E., Creed, I. F. and Trick, C. G. (2021) Lake browning may fuel phytoplankton biomass and trigger shifts in phytoplankton communities in temperate lakes. *Aquat. Sci.*, **83**, 1–15. https://doi.org/10.1007/s00027-021-00780-0.

Šimek, K., Pernthaler, J., Weinbauer, M. G., Hornák, K., Dolan, J. R., Nedoma, J., Masín, M. and Amann, R. (2001) Changes in bacterial community composition and dynamics and viral mortality rates associated with enhanced flagellate grazing in a mesoeutrophic reservoir. *Appl. Environ. Microbiol.*, **67**, 2723–2733. https://doi.org/10.1128/AEM.67.6.2723-2733.2001.

Šimek, K., Horňák, K., Jezbera, J., Nedoma, J., Vrba, J., Straškrábová, V., Macek, M., Dolan, J. R. and Hahn, M. W. (2006) Maximum growth rates and possible life strategies of different bacterioplankton groups in relation to phosphorus availability in a freshwater reservoir. *Environ. Microb.*, **8**, 1613–1624.

Sommer, U., Adrian, R., De Senerpont Domis, L., Elser, J. J., Gaedke, U., Ibelings, B., Jeppesen, E., Lurling, M. *et al.* (2012) Beyond the plankton ecology group (PEG) model: mechanisms driving plankton succession. *Annu. Rev. Ecol. Evol. and Syst.*, **43**, 429–448. https://doi.org/10.1146/annurev-ecolsys-110411-160251.

Sommer, U., Gliwicz, Z. M., Lampert, W. and Duncan, A. (1986) The PEG-model of seasonal succession of planktonic events in fresh waters. *Arch. Hydrobiol.*, **106**, 433–471. https://doi.org/10.1127/archiv-hydrobiol/106/1986/433.

Sterner, R. W. and Elser, J. J. (2002) Ecological stoichiometry: the biology of elements from molecules to the biosphere. In *Ecological Stoichiometry*, Princeton University Press, Princeton, New Jersey.

Stoecker, D. K., Hansen, P. J., Caron, D. A. and Mitra, A. (2017) Mixotrophy in the marine plankton. *Annu. Rev. Mar.*, **9**, 311–335. https://doi.org/10.1146/annurev-marine-010816-060617.

Tranvik, L. J. (1988) Availability of dissolved organic carbon for planktonic bacteria in oligotrophic lakes of differing humic content. *Microb. Ecol.*, **16**, 311–322. https://doi.org/10.1007/BF02011702.

Unrein, F., Massana, R., Alonso-Sáez, L. and Gasol, J. M. (2007) Significant year-round effect of small mixotrophic flagellates on bacterioplankton in an oligotrophic coastal system. *Limnol. Oceanogr.*, **52**, 456–469. https://doi.org/10.4319/lo.2007.52.1.0456.

Vasconcelos, F. V., Diehl, S., Rodríguez, P., Karlsson, J. and Byström, P. (2018) Effects of terrestrial organic matter on aquatic primary production as mediated by pelagic-benthic resources fluxes. *Ecosystems*, **21**, 1255–1268. https://doi.org/10.1007/s10021-017-0217-x.

Vasconcelos, F. R., Diehl, S., Rodríguez, P., Hedström, P., Karlsson, J. and Byström, P. (2019) Bottom-up and top-down effects of browning and warming on shallow lake food webs. *Glob. Change Bio.*, **25**, 504–521.

Vrede, T. (1998) Elemental composition (C: N: P) and growth rates of bacteria and Rhodomonas grazed by Daphnia. *J. Plankton Res.*, **20**, 455–470.

Wilken, S., Soares, M., Urrutia-Cordero, P., Ratcovich, J., Ekvall, M. K., Van Donk, E. and Hansson, L. A. (2018) Primary producers or consumers? Increasing phytoplankton bacterivory along a gradient of lake warming and browning. *Limnol. Oceanogr.*, **63**, S142–S155. https://doi.org/10.1002/lno.10728.

Wilken, S., Wiezer, S., Huisman, J. and Van Donk, E. (2010) Microcystins do not provide anti-herbivore defence against mixotrophic flagellates. *Aquat. Microb. Ecol.*, **59**, 207–216. https://doi.org/10.3354/ame01395.

Williamson, C. E., Overholt, E. P., Pilla, R. M., Leach, T. H., Brentrup, J. A., Knoll, L. B., Mette, E. M. and Moeller, R. E. (2015) Ecological consequences of long-term browning in lakes. *Sci. Rep.*, **5**, 18666. https://doi.org/10.1038/srep18666.

Journal of Plankton Research, 2025, Vol. 47, No. 1, fbae066
https://doi.org/10.1093/plankt/fbae066
Original Article